TH/P8-2

ITER Simulations with Internal and Edge Transport Barriers

T. Onjun 1), G. Bateman 2), A. Pankin 2), A.H. Kritz 2), V. Parail 3)

[1] *Sirindhorn International Institute of Technology, TU, Pathumthani, Thailand*
[2] *Department of Physics, Lehigh University, Bethlehem, PA, USA*
[3] *EURATOM/UKAEA Fusion Association, Culham Science Centre, Abingdon OX14 3DB, UK*

E-mail: thawatchai@siit.tu.ac.th

Abstract. Simulations of ITER with the presence of both an edge transport barrier (ETB) and an internal transport barrier (ITB) are carried out using the BALDUR integrated predictive modeling code. In these simulations, the height of the ETB or the top of the pedestal is calculated using the pedestal temperature model based on the magnetic and flow shear stabilization concept together with the infinite-*n* ballooning stability concept. A version of the semi-empirical Mixed Bohm/gyroBohm (Mixed B/gB) core transport model that includes ITB effects is used to compute the evolution of plasma profiles. In this model, the anomalous transport in the core can be stabilized by the influence of $E_r \times B$ flow shear and magnetic shear. The combination of Mixed B/gB transport model with ITB effects together with the pedestal model is used to simulate the time evolution of temperature, density, and current profiles for ITER discharges. The presence of both internal and edge transport barriers results in complicated scenarios that yield improved performance compared with standard *H*-mode discharges. It is found that the formation of an ITB has a strong impact on both temperature profiles, especially near the center of the plasma.

1. Introduction

The concept of magnetic confinement fusion has long been explored to address the feasibility of nuclear fusion energy. The International Thermonuclear Experimental Reactor (ITER) is an international collaborative effort with the objective of demonstrating the scientific and technological feasibility of nuclear fusion [1]. The goal of ITER is to produce plasmas with a sufficiently high fusion energy density for a long enough time to achieve a sustained fusion burn. Producing a significant fusion reaction rate inside a tokamak requires the ability to heat and contain high-temperature plasmas. Since the high confinement mode (*H*-mode) discharges in tokamaks generally provide excellent energy confinement and have acceptable particle transport rates for impurity control, fusion experiments such as ITER are designed to operate in the *H*-mode regime. The improved performance of *H*-mode mainly results from the formation of an edge transport barrier (ETB) [2], called the pedestal. In addition, it is known that the performance of an *H*-mode discharge can be further improved with the formation of a transport barrier inside the plasma, called an internal transport barrier (ITB) [3]. The presence of both edge and internal transport barriers, results in a scenario that yields higher plasma temperatures and fusion power production.

Predictions of ITER performance have been carried out for a variety of scenarios using various integrated modeling codes [4-10]. For example, the BALDUR integrated predictive modeling code [11] was used to predict the performance of ITER for the standard *H*-mode scenario [4, 6-

8]. The performance of ITER was evaluated in terms of the fusion power production and the fusion Q, which is the ratio of fusion power (to neutrons and alpha particles) to the applied heating power. A range of performance is predicted, depending on the choice of plasma density, heating power, impurity concentration and assumptions about the models employed in the simulations. It was found that the predicted performance of ITER with the Mixed Bohm/gyroBohm (Mixed B/gB) transport model is relatively low compared to those using other transport models. It is worth noting that the Mixed B/gB model was developed using simulations of JET plasma discharges. Another remark is that in previous studies, the effects of ITBs were not included in the simulations, and the present work is motivated by the need to explore ITER scenarios that include ITBs in *H*-mode discharges.

In this paper, a preliminary study of ITER simulations is presented that includes the effects of an internal transport barrier together with the *H*-mode edge transport barrier. The ETB is described in terms of a pedestal model based on magnetic and flow shear stabilization, together with limits imposed by a ballooning mode instability. In simulations of discharges that contain an ITB, the ITB is formed by the suppression of core anomalous transport. This paper is organized as follows: brief descriptions relevant components of the BALDUR code, the anomalous transport model, and the pedestal model are presented in Section 2; predictions of ITER performance using the BALDUR code are described in Section 3; and a summary is given in Section 4.

2. BALDUR Integrated Predictive Modeling Code

The BALDUR integrated predictive modeling code is used to compute the time evolution of plasma profiles including electron and ion temperatures, deuterium and tritium densities, helium and impurity densities, magnetic q, neutrals, and fast ions. These time-evolving profiles are computed in the BALDUR code by combining the effects of many physical processes self-consistently, including the effects of transport, plasma heating, particle influx, boundary conditions, the plasma equilibrium shape, and sawtooth oscillations. Fusion heating and helium ash accumulation are also computed self-consistently. BALDUR simulations have been intensively compared with a wide variety of plasma experimental data, which yield an overall agreement with about a 10% relative RMS deviation [12, 13]. In the BALDUR code, fusion heating power is determined by the nuclear reaction rates together with a Fokker Planck package used to compute the slowing down spectrum of fast alpha particles on each flux surface in the plasma. The fusion heating component of the BALDUR code also computes the rate of the production of thermal helium ions and the rate of the depletion of deuterium and tritium ions within the plasma core. The effect of sawtooth oscillation is taken into account using the Porcelli sawtooth model [14] to trigger sawtooth crashes and a modified Kadomtsev magnetic reconnection model [15] to describe the effects of each sawtooth crash.

2.1 ITB model

In this work, an ITB is formed by the suppression of core anomalous transport due to ω_{ExB} flow shear and magnetic shear. This effect is included in the Mixed Bohm/gyro-Bohm (Mixed B/gB) anomalous core transport model [16]. This core transport model is an empirical model. It was originally a local transport model with Bohm scaling. A transport model is said to have “Bohm” scaling when the transport diffusivities are proportional to the gyro-radius times thermal velocity. Transport diffusivities in models with Bohm scaling are also functions of the profile shapes (characterized by normalized gradients) and other plasma parameters such as magnetic q. These

parameters are held fixed in systematic scans in which only the gyro-radius is changed relative to plasma dimensions. The original model was subsequently extended to describe ion transport, and a gyro-Bohm term was added in order to produce simulation results that match data from smaller tokamaks as well as data from larger machines. A transport model is said to have "gyro-Bohm" scaling when the transport diffusivities are proportional to the square of the gyro-radius times thermal velocity divided by a plasma linear dimension such as the major radius. The Bohm contribution to the original model usually dominates over most of the plasma. The gyro-Bohm contribution usually makes its largest contribution in the deep core of the plasma and it plays a significant role only in smaller tokamaks with relatively low heating power and low magnetic field. To include the ITB effect, the Bohm contribution is modified by a cut-off that is a function of magnetic and flow shear. The Bohm/gyro-Bohm transport model with ITB effect included [17] can be expressed as follows:

$$\chi_e = 1.0\chi_{gB} + 2.0\chi_B$$

$$\chi_i = 0.5\chi_{gB} + 4.0\chi_B + \chi_{neo}$$

$$D_H = D_Z = \left[0.3 + 0.7\rho\right]\frac{\chi_e\chi_i}{\chi_e + \chi_i}$$

where

$$\chi_{gB} = 5\times10^{-6}\sqrt{T_e}\left|\frac{\nabla T_e}{B_\phi^2}\right|$$

$$\chi_B = 4\times10^{-5}R\left|\frac{\nabla\left(n_eT_e\right)}{n_eB_\phi}\right|q^2\left(\frac{T_{e,0.8}-T_{e,1.0}}{T_{e,1.0}}\right)\Theta\left(-0.14+s-\frac{1.47\varpi_{E\times B}}{\gamma_{ITG}}\right).$$

In these expressions, the χ_e is the electron diffusivity, χ_i is the ion diffusivity, D_H is the particle diffusivity, D_z is the impurity diffusivity, χ_{gB} is the gyro-Bohm contribution, χ_B is the Bohm contribution, ρ is normalized minor radius, T_e is is the local electron temperature in keV, B_φ is the toroidal magnetic field, R is the major radius, n_e is the local electron density, q is the safety factor, s is the magnetic shear $[r\,(\mathrm{d}\,q\,/\,\mathrm{d}r)\,/\,q]$, ω_{ExB} is the flow shearing rate and the γ_{ITG} is the ITG growth rate, estimated as v_{ti}/qR, in which v_{ti} is the ion thermal velocity.

2.2 ETB models

In the BALDUR code, the outer plasma boundary condition is set at the top of the pedestal. As a result, the code requires a model for both temperature and density at the top of the pedestal. A simple model for estimating pedestal temperature has been developed by using the values of pedestal width and pedestal pressure gradient [18]. In the present work, the pedestal width is estimated using a magnetic and flow shear stabilization concept ($\Delta = C_w\rho s^2$) [19] and the pedestal gradient is estimated using a first ballooning mode pressure gradient limit. The effect of the bootstrap current and plasma geometry are also considered. The pedestal temperature takes the following form:

$$T_{\mathrm{ped}}\left(keV\right) = 0.323C_W^2\left(\frac{B_T}{q^2}\right)^2\left(\frac{M_i}{R^2}\right)\left(\frac{\alpha_c}{n_{\mathrm{ped},19}}\right)^2 s^4$$

where $n_{\mathrm{ped},19}$ is the electron density at the top of the pedestal in units of 10^{19} m^{-3}. The expression used to compute the normalized critical pressure gradient, α_c, and the calibration used to determine

the constant C_W (=2.42) are described in Ref. [18]. In general, the pedestal density (n_{ped}) in *H*-mode plasmas is a large fraction of line average density (n_l). Here the pedestal density is taken to be

$$n_{ped} = 0.71 n_l$$

based on the model employed in Ref. [4].

3. Results and Discussions

The BALDUR code is used to carry out simulations of ITER with the design parameters for full-current *H*-mode discharges (R = 6.2 m, a = 2.0 m, I_p = 15 MA, B_T = 5.3 T, κ_{95} = 1.7, δ_{95} = 0.33 and $n_l = 1.0 \times 10^{20}$ m^{-3}). In the simulations, the plasma current and density are ramped up to the target values within the first 100 seconds of the simulation. The plasma current during the start up phase is initially 3 MA and is slowly increased with the rate of 0.12 MA/sec to the target current. It is found, using the PEDESTAL module [20], that the plasma makes a transition to the H-mode phase at 2 sec during this startup ramp. It is worth noting that there are several physical processes that have not been included in these simulations, such as ELM crashes and neoclassical tearing modes. Consequently, the simulation results do not represent the complete dynamic behavior of the ITER plasma. However, it is expected that these simulations include enough physics to describe the plasma when it reaches a quasi-steady state with sawtooth oscillations. The simulations yield complex and interesting interactions within the plasma itself — such as the self heating of the plasma by the production of fast alpha particles and redistribution of heating power after each sawtooth crash. Sawtooth oscillations are considered during the time interval between 10 sec and 995 sec. For each simulation, anomalous transport is calculated using either the Mixed B/gB transport model or the MMM95 transport model, while neoclassical transport is computed using the NCLASS module [21]. The boundary conditions are provided at the top of the pedestal by the pedestal model and will be varied later in this paper in order to examine the sensitivity of the results to the pedestal temperature. It is assumed that the electron and ion pedestal temperatures have the same values. In these simulations, the auxiliary heating power is 40 MW, which is comprised of a combination of 33 MW NBI heating power together with 7 MW of RF heating power. As noted above, the Porcelli sawtooth model is used to trigger sawtooth crashes and a modified Kadomtsev magnetic reconnection model is used to compute the effects of each sawtooth crash. Note that during each sawtooth crash, it is assumed that 10% of magnetic flux is mixed to describe the effect of sawtooth crash.

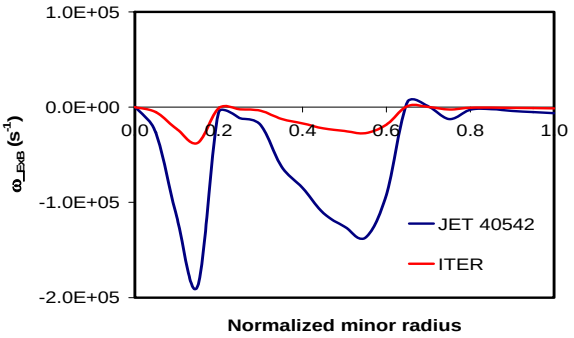

Fig. 1: The ω_{ExB} profiles for JET discharge 40452 and ITER are plotted as a function of a normalized minor radius at time. The value for ITER is assumed to be 20% of the value for JET discharge 40452.

During the slow current ramp (reaching the target value in 100 sec), the plasma density is also ramped up to the final plasma density during while the full heating power is applied starting from the beginning of the simulation. During this ramp, the plasma makes a transition from *L*-mode to *H*-mode. Since there is a strong heating early in the simulations, all the simulations enter the

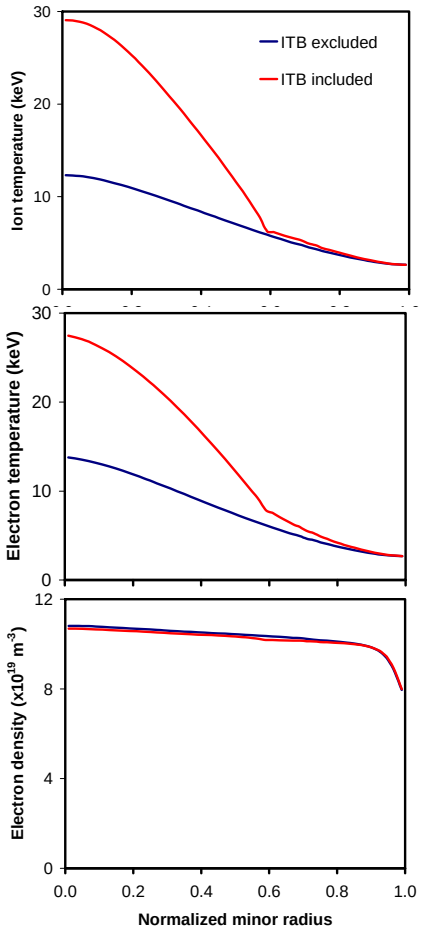

Fig. 2: Profiles for ion temperature (top) and electron temperature (middle) and electron density (bottom) are plotted as a function of a normalized minor radius at time of 1000 sec. The simulations are carried out with and without) ITB effects

H-mode phase approximately within 2 sec. In Fig. 1, the ω_{ExB} flow shear profile for an optimized magnetic shear discharge in the Joint European Torus (JET), discharge 40542, is shown. In this work, the ω_{ExB} profile for ITER is taken to be 20% of that for the JET discharge 40542. The reduction in the flow shear rate was chosen to approximate the effect of the reduced momentum carried by the 1 MeV neutral beams in ITER, compared with the 1 keV beams in JET, and the higher density in the ITER experiment compared with that in the JET experiment. As a result of these two effects, it is more difficult to produce the magnitude of the ω_{ExB} flow shear found in the JET experiment.

The profiles for ion temperature (top), electron temperature (middle) and electron density (bottom) are shown in Fig. 2 as a function of normalized minor radius at a time of 1000 sec. These results are shown for simulations that are carried out using the Mixed B/gB model with the effects of ITB excluded (blue) and included (red). When ITB effects are included in the transport model, the central temperature increases significantly, while the edge temperature remains unchanged. It is found that the pedestal boundary condition remains almost constant after the density reaches its target value. Note that the ion pedestal temperature is assumed to be the same as the electron pedestal temperature in this model. Also, the effects of ELMs have not been included in these simulations. For the electron density, the core profile is nearly flat, with relatively limited central peaking. When an ITB is included, the central density profile remains nearly unchanged. In addition, it is found that the ITB extends to a plasma radius of up to $\rho = 0.6$. This ITB region results from the reduction of transport in the region close to the plasma core, which can be seen in figure 3.

Summaries of the central and pedestal temperatures and densities predicted by these two simulations are shown in Table 1. It can be seen that the central ion temperature increases significantly when the ITB effects are included. The central ion temperature in the ITB simulation is about 29.1 keV, which is in the most effective range for fusion power production. The central ion and electron temperatures increase by 137% and 99%, respectively when simulations with ITB effects are compared with simulations without ITB effects. This increase of central temperature has a strong impact on the total plasma stored energy and the nuclear fusion power production.

The total plasma stored energy is shown as a function of time between 900 sec to 1000 in Fig. 4. It can be seen that the value of plasma stored energy is in the range of 200 MJ for the simulation with no ITB, while the plasma stored energy increases to 300 MJ in the simulation with ITB effects included.

There are two types of auxiliary heating used in the ITER simulation. The total amount of neutral beam injection heating power, P_{NBI}, is 33 MW. Another source of auxiliary heating is the RF heating. The total amount of RF heating power is 7 MW. For simplicity, the RF heating profiles are taken to have a parabolic shape, although it is recognized that the physics of RF heating is likely to be more complicated in the ITER plasma. The power deposition profiles are shown in Fig. 5 for a simulation without ITB effects (left) and with ITB effects (right). Note that Ohmic heating is small compared to other types of heating. The alpha heating power deposition profile is also shown in Fig. 5. It is found that the alpha heating power is the main heating source of the plasma in the simulation with ITB effects. However, the alpha power heating is only slightly higher than the combined electron and ion NBI heating power in the simulation without ITB effects.

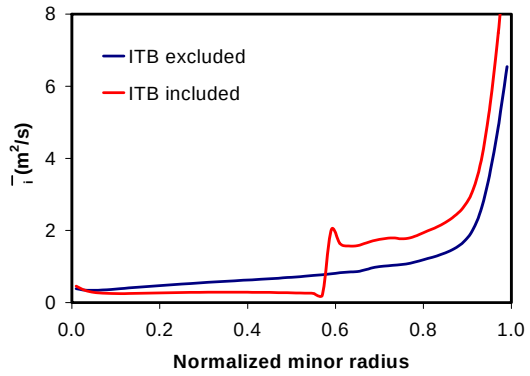

Fig. 3: The profile of total ion diffusivity is plotted as a function of normalized minor radius at time of 1000 sec. The simulations are carried out with and without ITB effects.

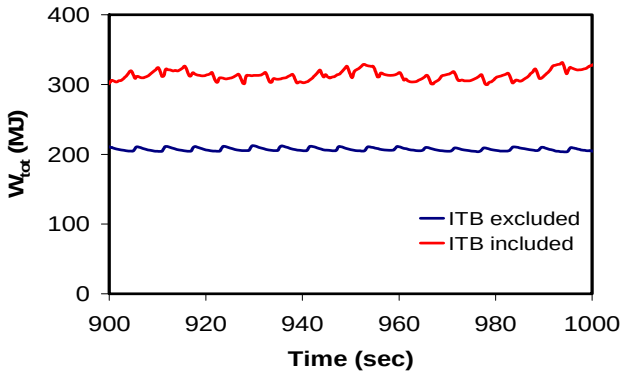

Fig. 4: The plasma stored energy is plotted as a function of time for simulations with ITB effects excluded and included.

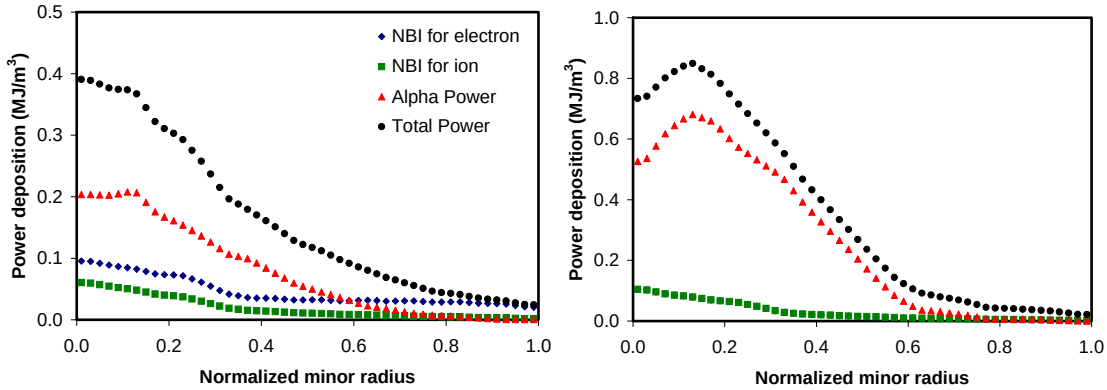

Fig. 5: The power deposition profiles are shown as a function of normalized minor radius for the simulations with ITB effects excluded (left) and included (right).

Table 1: Summary of central and pedestal temperatures and density at the time of 1000 sec.

Parameters	Unit	ITB excluded	ITB included
$T_{i,0}$	keV	12.3	29.1
$T_{e,0}$	keV	13.8	27.5
$n_{e,0}$	10^{19} m^{-3}	10.8	10.7
T_{ped}	keV	2.6	2.6
$n_{e,ped}$	10^{19} m^{-3}	7.1	7.1

The time-dependence of the alpha power deposition is shown in Fig. 6 from the simulations with ITB effects excluded (blue curve) and included (red curve). It can be seen that the alpha power from the simulation with ITB effects included is much higher than that without an ITB. The average of alpha power during the time between 900 sec and 1000 sec is summarized in Table 2. The fusion performance can be evaluated in term of the fusion Q, which can be calculated as

$$\text{Fusion } Q = \frac{5 \times P_{\alpha,avg}}{P_{AUX}},$$

where $P_{\alpha,avg}$ is a time-average of the alpha power and P_{AUX} is the auxiliary heating power (equal to 40 MW for these simulations). It can be seen in Table 2 that the fusion Q increases by 200% when ITB effects are included.

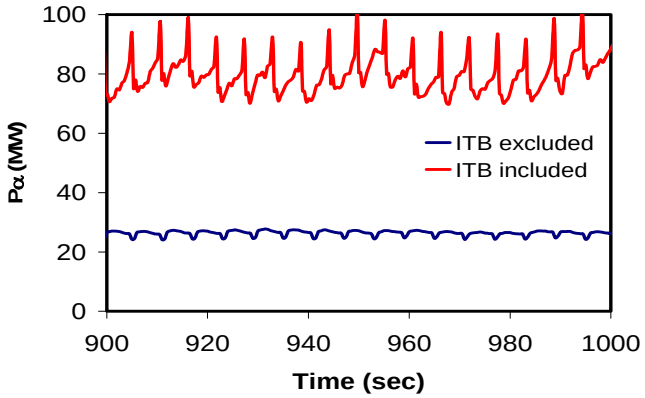

Fig. 6: The alpha power production is plotted as a function of time for the simulation when an ITB is included (red) and excluded (blue).

Table 2: Summary of average alpha heating power and corresponding fusion Q.

Parameters	Unit	ITB excluded	ITB included
$P_{\alpha,\,avg}$	MW	26.4	79.5
Fusion Q		3.3	9.9

4. Summary

Self-consistent modeling of the ITER tokamak has been carried out using the BALDUR code. The outer plasma boundary in these simulations is taken to be at the top of the pedestal, where the pedestal temperatures and density are computed using a theory-based pedestal model. The pedestal temperature model is based on magnetic and flow shear stabilization of transport

together with the first stability regime of a ballooning mode limit. The pedestal temperature model is used together with a Mixed B/gB core transport model, which can include the effects of an ITB. It is found that the formation of an ITB has a strong impact on both electron and ion temperature profiles, especially near the center of the plasma. When the effect of an ITB is not included, the predicted central ion temperature is about 12.3 keV. With an ITB included in the simulation, the central ion temperature increases by more than a factor of two. The increase of central temperature results in a significant improvement in the alpha power production and, consequently, in the fusion performance. It is observed that in most of the plasma core in these ITER simulations, the ion and electron thermal and particle diffusivities are smaller with an ITB included than in those without the ITB. This reduction in the diffusivity results in stronger gradients and, consequently, higher values of the central temperature and density.

5. Acknowleagement

This work is supported by Commission on Higher Education (CHE) and the Thailand Research Fund (TRF) under Contract No. RMU5180017.

6. References

[1] Aymar R *et al.*, 2002 Plasma Phys. Control. Fusion **44** 519
[2] Hubbard A, 2000 Plasma Phys. Control. Fusion **42** A15
[3] Connor J W *et al.*, 2004 Nucl. Fusion **44** R1
[4] Bateman G *et al.*, 2003 Plasma Phys. Control. Fusion **45** 1939
[5] Onjun T *et al.*, 2005 Phys. Plasmas **12** 082513
[6] Onjun T *et al.*, 2008 J. of Physics: Conference Series **123** 012034
[7] Tharasrisuthi K *et al*., 2008 Thammasat International Journal of Science and Tech. **13** 45
[8] Picha R *et al.*, 2008 Proc. 35th EPS Conf on Plasma Physics, Hersonissos 9-13 June 2008
[9] Halpern, F.D. et al., 2008, Phys. Plasmas 15 062505
[10] Budny, R.V. et al., 2008 Nucl. Fusion 48 075005
[11] Singer C E *et al.*, 1988 Comput. Phys. Commun. **49** 399
[12] Hannum D *et al.*, 2001 Phys. Plasmas **8** 964
[13] Onjun T *et al.*, 2001 Phys. Plasmas **8** 975
[14] Porcelli F *et al.*, 1996 Plasma Phys. Control. Fusion **38** 2163
[15] Bateman G *et al.*, 2006 Phys. Plasmas **13** 072505
[16] Erba M *et al.*, 1997 Plasma Phys. Control. Fusion **39** 261
[17] Tala T J J, *et al*., 2001 Phys. Control. Fusion **43** 507
[18] Onjun T *et al.*, 2002 Phys. Plasmas **9** 5018
[19] Sugihara M *et al.,* 2000 Nucl. Fusion **40** 1743
[20] Kritz A *et al*., 2004 Comput. Phys. Comm., **164**, 108; http://w3.pppl.gov/NTCC
[21] Houlberg W A *et al.*, 1997 Phys. Plasmas **4** 3231